

# Pattern description of the ground state properties of the one-dimensional axial next-nearest-neighbor Ising model in a transverse field

Yun-Tong Yang<sup>1,2</sup> and Hong-Gang Luo<sup>1,2,3,\*</sup>

<sup>1</sup>*School of Physical Science and Technology, Lanzhou University, Lanzhou 730000, China*

<sup>2</sup>*Lanzhou Center for Theoretical Physics & Key Laboratory of Theoretical Physics of Gansu Province, Lanzhou University, Lanzhou 730000, China*

<sup>3</sup>*Beijing Computational Science Research Center, Beijing 100084, China*

The description and understanding of the consequences of competing interactions in various systems, both classical and quantum, are notoriously difficult due to insufficient information involved in conventional concepts, for example, order parameters and/or correlation functions. Here we go beyond these conventional language and present a pattern picture to describe and understand the frustration physics by taking the one-dimensional (1D) axial next-nearest-neighbor Ising (ANNNI) model in a transverse field as an example. The system is dissected by the patterns, obtained by diagonalizing the model Hamiltonian in an operator space with a finite lattice size  $4n$  ( $n$ : natural number) and periodic boundary condition. With increasing the frustration parameter, the system experiences successively various phases/metastates, identified respectively as those with zero, two, four,  $\dots$ ,  $2n$  domains/kinks, where the first is the ferromagnetic phase and the last the antiphase. Except for the ferromagnetic phase and antiphase, the others should be metastates, whose transitions are crossing over in nature. The results clarify the controversial issues about the phases in the 1D ANNNI model and provide a starting point to study more complicated situations, for example, the frustration systems in high dimensions.

*Introduction.*—Frustration arisen geometrically [1] or interactionally [2–4], on the one hand, fascinates the competition between different states of the system, resulting in notorious difficulties in describing its fundamental properties even in the most simple situation, for example, the antiferromagnetically coupled Ising spins on a triangle; on the other hand, many exotic states emerge out of the conventional framework of many-body physics. This kind of competing interaction has already been seen in the transverse antiferromagnetic Ising model with a longitudinal magnetic field applied, in which the competition between the longitudinal field and the antiferromagnetic interaction leads to mixed-order phase transition [5–10], a concept not defined well.

A direct competition between exchange interactions has been introduced in the axial next-nearest-neighbor Ising (ANNNI) model [11–14], namely, the nearest-neighbor ferromagnetic interaction  $J_1 (> 0)$  competes with the next nearest-neighbor antiferromagnetic one  $J_2 (< 0)$ , defining a frustration parameter  $\kappa = -J_2/J_1$ . The addition of the frustration complicates dramatically the situation: only consensus obtained by different ways, both analytical and numerical, is the case of weak frustration, in which the system is in the ferromagnetic phase. Otherwise, the conclusions are diverse [15–18]. We first come to the high frustration side,  $\kappa > 0.5$ . An antiferromagnetism was concluded by using bosonization technique and a renormalization group analysis in relationship to the anisotropic Heisenberg spin-1/2 chain [19], which is in sharp contrast to the antiphase obtained by other investigations. Moving to the intermediate frustration and finite transverse field, the statements about the phases and phase transitions are quite controversial,

even contradictory. For example, two additional phases, paramagnetic and floating phases have been addressed [20–22], and the paramagnetic phase was further divided into unmodulated (I) and modulated (II) ones [15, 23–26]. However, a quantum fidelity approach gave an infinite number of modulated phases in this regime as the thermodynamical limit was considered [18]. The floating phase was even absent in the studies of the interface approach [27] and the finite-size scaling [28]. It is also controversial about the phase boundaries. While these two ferromagnetic-paramagnetic I and floating-antiphase transitions are of second-order, the floating-paramagnetic II phase transition is considered as infinite order, i.e., the Kosterlitz-Thouless transition [29]. On the contrary, the transition lines separating the infinite modulated phases are of second-order, and the line between the floating and the antiphases is possibly of first-order [18]. It seems that the number, nature, or location of the phases are dependent of the approaches used. On the one hand, this indicates the fact that the frustration is indeed notoriously difficult in nature, which refuses a complete theoretical description, and on the other hand, the conventional approaches developed up to date are at least insufficient as encountering the physics involving the frustration. Therefore, it is desirable to develop an effective way to tackle the frustration physics.

In the present work we employ a pattern formulation to discuss the frustration physics involved in the ANNNI model. For the sake of clarity, we limit ourselves to the one-dimensional (1D) case and to a finite chain size, where all spectra of the model are readily obtained and the ground state can be analyzed in detail. The patterns obtained are not different to those obtained in the

transverse Ising model [30], but their eigenenergies intersect with the change of frustration parameter  $\kappa$ , quite different to the non-frustrated cases. We identify which patterns are involved in the phases of the ANNNI model and how they evolve with the changes of the frustration parameter  $\kappa$ : at low frustration, the ferromagnetic pattern  $\lambda_1$  dominates over the others, and increasing  $\kappa$ , the patterns  $\lambda_{2,3}$  with two domains/kinks replace the pattern  $\lambda_1$ , dominating the ground state of the system. And then, the patterns  $\lambda_{4,5}$  come into play, in replace of the patterns  $\lambda_{2,3}$ . In the case of  $L = 8$  this comes to the final patterns (the antiphase) dominant over the others in the high frustration situation. For  $L = 12$  the rule remains valid, but they are the patterns  $\lambda_{6,7}$  representing the antiphase. Between the ferromagnetic phase and the antiphase, it is a crossover, rather than certain phases, because of the absence of clear order parameters or associated broken symmetries. In the following we explore in detail our statement.

*Model and Method.*—The Hamiltonian of the ANNNI model with a transverse field reads

$$\hat{H}' = -J'_1 \sum_{\langle i,j \rangle} \hat{\sigma}_i^z \hat{\sigma}_j^z + J'_2 \sum_{\langle\langle i,j \rangle\rangle} \hat{\sigma}_i^z \hat{\sigma}_j^z - g \sum_i \hat{\sigma}_i^x, \quad (1)$$

where  $\langle i,j \rangle$  and  $\langle\langle i,j \rangle\rangle$  represent the nearest-neighbor ferromagnetic and next nearest-neighbor antiferromagnetic exchange interactions of the spin located at sites  $i$  and  $j$ , respectively.  $J'_1$  and  $J'_2$  are non-negative.  $g$  is the transverse field, which is taken as units of energy. Thus Eq. (1) is reformulated as  $\hat{H}' = \frac{g}{2} \hat{H}$ , where

$$\hat{H} = -J \sum_{\langle i,j \rangle} (\hat{\sigma}_i^z \hat{\sigma}_j^z + \hat{\sigma}_j^z \hat{\sigma}_i^z) + \kappa J \sum_{\langle\langle i,j \rangle\rangle} (\hat{\sigma}_i^z \hat{\sigma}_j^z + \hat{\sigma}_j^z \hat{\sigma}_i^z) - 2 \sum_i \hat{\sigma}_i^x. \quad (2)$$

Here  $J = J'_1/g$  and  $\kappa J = J'_2/g$ . For simplicity, we limit ourselves to the 1D case, though it is straightforward to extend to high dimensions. For the chain length  $L$  with periodic boundary condition (PBC), the model Hamiltonian can be rewritten as

$$\hat{H} = \begin{pmatrix} -i\hat{\sigma}_1^y & \hat{\sigma}_1^z & -i\hat{\sigma}_2^y & \hat{\sigma}_2^z & -i\hat{\sigma}_3^y & \hat{\sigma}_3^z & \dots & -i\hat{\sigma}_L^y & \hat{\sigma}_L^z \end{pmatrix} \times \begin{pmatrix} 0 & -1 & 0 & 0 & 0 & 0 & \dots & 0 & 0 \\ -1 & 0 & 0 & -J & 0 & \kappa J & \dots & 0 & -J \\ 0 & 0 & 0 & -1 & 0 & 0 & \dots & 0 & 0 \\ 0 & -J & -1 & 0 & 0 & 0 & \dots & 0 & \kappa J \\ 0 & 0 & 0 & 0 & 0 & 0 & \dots & 0 & 0 \\ 0 & \kappa J & 0 & 0 & 0 & 0 & \dots & 0 & 0 \\ \vdots & \vdots & \vdots & \vdots & \vdots & \vdots & \ddots & \vdots & \vdots \\ 0 & 0 & 0 & 0 & 0 & 0 & \dots & 0 & -1 \\ 0 & -J & 0 & \kappa J & 0 & 0 & \dots & -1 & 0 \end{pmatrix} \times (i\hat{\sigma}_1^y \hat{\sigma}_1^z \ i\hat{\sigma}_2^y \hat{\sigma}_2^z \ i\hat{\sigma}_3^y \hat{\sigma}_3^z \ \dots \ i\hat{\sigma}_L^y \hat{\sigma}_L^z)^T, \quad (3)$$

where the identity of Pauli matrices  $\hat{\sigma}^y \hat{\sigma}^z = i\hat{\sigma}^x$  has been used for each site  $i$  and the matrix in Eq. (3) has dimen-

Pattern $\lambda_1$	(-,-)	(-,-)	(-,-)	(-,-)	(-,-)	(-,-)	(-,-)	(-,-)	(-,-)	(-,-)	(-,-)
Pattern $\lambda_{2,3}$	(-,-)	(-,-)	(-,-)	(-,-)	(-,-)	(-,+)	(-,+)	(-,+)	(-,+)	(-,+)	(-,+)
Pattern $\lambda_{4,5}$	(-,-)	(-,-)	(-,-)	(+,+)	(+,+)	(+,+)	(-,+)	(-,+)	(-,+)	(+,+)	(+,+)
Pattern $\lambda_{6,7}$	(-,-)	(-,-)	(+,+)	(+,+)	(-,+)	(-,+)	(+,+)	(-,+)	(-,+)	(+,+)	(+,+)
Pattern $\lambda_{8,9}$	(-,-)	(+,+)	(+,+)	(-,+)	(+,+)	(+,+)	(-,+)	(+,+)	(+,+)	(-,+)	(+,+)
Pattern $\lambda_{10,11}$	(-,-)	(+,+)	(-,+)	(-,+)	(+,+)	(-,+)	(+,+)	(-,+)	(+,+)	(-,+)	(+,+)
Pattern $\lambda_{12}$	(-,+)	(+,+)	(+,+)	(-,+)	(+,+)	(-,+)	(+,+)	(-,+)	(+,+)	(-,+)	(+,+)
Pattern $\lambda_{13}$	(-,+)	(-,+)	(-,+)	(-,+)	(-,+)	(-,+)	(-,+)	(-,+)	(-,+)	(-,+)	(-,+)
Pattern $\lambda_{14,15}$	(-,+)	(-,+)	(-,+)	(-,+)	(-,+)	(-,+)	(-,+)	(-,+)	(-,+)	(-,+)	(-,+)
Pattern $\lambda_{16,17}$	(-,+)	(-,+)	(-,+)	(-,+)	(-,+)	(-,+)	(-,+)	(-,+)	(-,+)	(-,+)	(-,+)
Pattern $\lambda_{18,19}$	(-,+)	(-,+)	(-,+)	(-,+)	(-,+)	(-,+)	(-,+)	(-,+)	(-,+)	(-,+)	(-,+)
Pattern $\lambda_{20,21}$	(-,+)	(-,+)	(-,+)	(-,+)	(-,+)	(-,+)	(-,+)	(-,+)	(-,+)	(-,+)	(-,+)
Pattern $\lambda_{22,23}$	(-,+)	(-,+)	(-,+)	(-,+)	(-,+)	(-,+)	(-,+)	(-,+)	(-,+)	(-,+)	(-,+)
Pattern $\lambda_{24}$	(-,+)	(-,+)	(-,+)	(-,+)	(-,+)	(-,+)	(-,+)	(-,+)	(-,+)	(-,+)	(-,+)

FIG. 1. The patterns and their relative phases obtained by the first diagonalization, marked by the single-body operators  $\hat{A}_n = \sum_{i=1}^L [u_{n,2i-1}(i\hat{\sigma}_i^y) + u_{n,2i}\hat{\sigma}_i^z]$  with  $(\pm, \pm)$  denoting the signs of  $(u_{n,2i-1}, u_{n,2i})$  for the 1D ANNNI model with  $L = 12$  under PBC. (The case of  $L = 8$  is the same as Fig. 1 in Ref. [30].) All patterns are divided into two groups marked by the red and blue dashed frames with  $\lambda_n < 0$  and  $\lambda_n > 0$ , respectively [see, Fig.2 (a)].

sion  $2L \times 2L$ . It can be diagonalized to obtain eigenvalues and corresponding eigenfunctions  $\{\lambda_n, u_n\}$  ( $n = 1, 2, \dots, 2L$ ), which define the patterns marked by  $\lambda_n$ . With these patterns at hand, the ANNNI Hamiltonian is rewritten as

$$\hat{H} = \sum_{n=1}^{2L} \lambda_n \hat{A}_n^\dagger \hat{A}_n, \quad (4)$$

where each pattern  $\lambda_n$  composes of single-body operators

$$\hat{A}_n = \sum_{i=1}^L [u_{n,2i-1}(i\hat{\sigma}_i^y) + u_{n,2i}\hat{\sigma}_i^z]. \quad (5)$$

The validity of Hamiltonian Eq. (4) can be confirmed by inserting into the complete basis  $|\{\sigma_i^z\}\rangle$  ( $i = 1, 2, \dots, L$ ) with  $\hat{\sigma}_i^z |\{\sigma_i^z\}\rangle = \pm_i |\{\sigma_i^z\}\rangle$ , as done in Refs.[30–32].

*Patterns and Solution.*—We firstly explore the properties of the patterns marked by the single-body operators  $\hat{A}_n$  involving the eigenfunctions  $u_n$ 's, shown as patterns in Fig. 1 and their amplitudes varying with the frustration parameter  $\kappa$  in Fig. 2 for  $L = 12$ . The other parameters used here and hereafter are  $g = J = 1$ . According to the behaviors of the eigenvalues shown in Fig. 2 (a), all patterns can be divided into two groups, one has negative eigenvalues  $\lambda_n < 0$ , as marked by red dashed frame, and the other has positive eigenvalues marked by blue dashed frame. There are  $L = 12$  pairs of signatures (plus and minus) for each pattern  $\lambda_n$ , which denote the relative phase of the eigenfunctions  $u_{n,2i-1}$  and  $u_{n,2i}$ . The characteristic features for the relative phases are the same as those

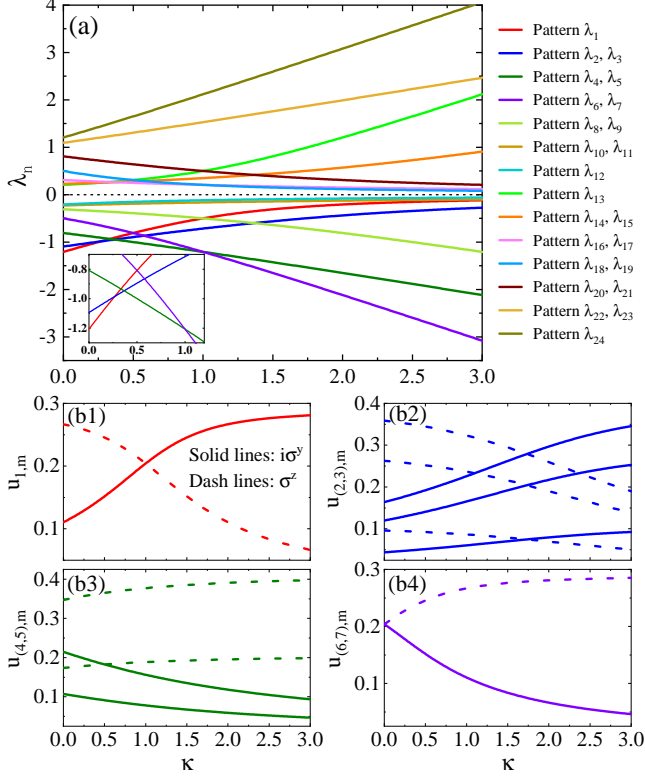


FIG. 2. (a) The eigenenergies of the patterns (colored solid lines) and (b) their eigenfunctions (color solid (dashed) lines for the  $i\hat{\sigma}^y$  ( $\hat{\sigma}^z$ ) components) as functions of the frustration parameter  $\kappa$  for  $L = 12$ . An enlarged view for first four low-energy patterns is shown in the inset. The eigenfunctions of the patterns  $\lambda_1, \dots, \lambda_7$  shown in (b) describe the weight changes of the  $i\hat{\sigma}^y$  and  $\hat{\sigma}^z$  in each pattern with components  $u_{n,m}$  ( $n$  denotes the pattern number and  $m$  its lattice components with some degeneracy). In addition, the eigenfunctions are free of a total phase factor  $e^{i\pi}$  but their relative phases remain fixed. The other parameters used here and hereafter are  $g = J = 1$

of  $L = 8$  in Ref. [30]. The difference is the eigenvalues of the patterns shown in Fig. 2 (a), in which the eigenvalues intersect: an enlarged view for four low-energy patterns is presented in the inset. This determines the dominant components of the ground state of the system, as discussed below.

After clarifying the pattern picture obtained, we solve Eq. (4) by inserting into the complete basis, as mentioned above. Firstly, one readily obtains the matrix  $[\hat{A}_n]_{\{\sigma_i^z\}, \{\sigma_i^z\}'}$  =  $\langle \{\sigma_i^z\} | \hat{A}_n | \{\sigma_i^z\}' \rangle$  and then Eq. (4) can be solved by diagonalizing the matrix with elements

$$\begin{aligned} \langle \{\sigma_i^z\} | \hat{H} | \{\sigma_i^z\}' \rangle &= \sum_{n=1}^{2L} \lambda_n \\ &\times \sum_{\{\sigma_i^z\}''} [\hat{A}_n^\dagger]_{\{\sigma_i^z\}, \{\sigma_i^z\}''} [\hat{A}_n]_{\{\sigma_i^z\}'', \{\sigma_i^z\}'}. \end{aligned} \quad (6)$$

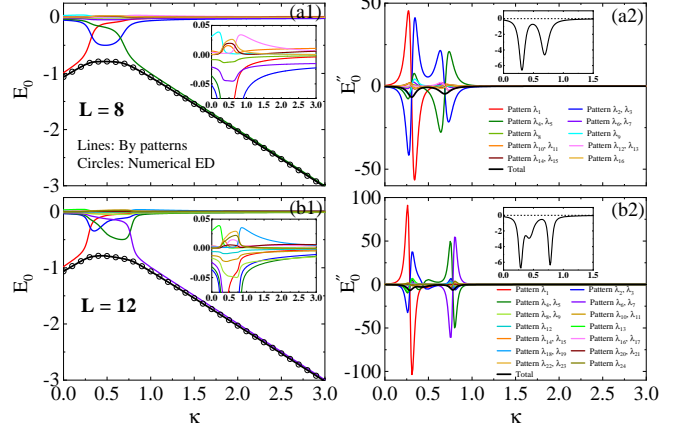


FIG. 3. (a1) & (b1) The ground state energies as functions of the frustration parameter  $\kappa$ , respectively, obtained by Eq. (4) (thick black solid lines) and numerical ED (circles). In addition, the energy components of the patterns (thin color solid lines) are also presented and the insets show the details near zero energy. (a2) & (b2) The second derivatives of the corresponding energy levels (thick black solid lines) and their pattern components (thin color solid lines). The insets are enlarged view of the second derivative of the total energies. The step of the frustration parameter  $\kappa$  is 0.003.

Figure 3 (a1) & (b1) present the results for the ground state as the function of the frustration parameter  $\kappa$  for  $L = 8$  and  $12$ , respectively, as shown by thick black solid lines. In order to confirm the validity of the pattern formulation, the results of direct exact diagonalization (ED) have also presented for comparison, shown as circles. The exact agreement between them from weak to strong frustration regimes is noticed, which is not surprising since no any approximation has been introduced.

*QPTs in the ANNNI model.*—The patterns obtained above provides insights on the QPTs involved in the ANNNI model, which is helpful to clarify the controversial issues. The ground state energies shown in Fig. 3 (a1) and (b1) are dominated by different patterns in different frustration parameters: (i) for low  $\kappa$ , the ground state is dominated by the pattern  $\lambda_1$ , which is identified as the ferromagnetic phase, in agreement with that of Ref. [30] for the model parameters we consider; (ii) increasing  $\kappa$ , the patterns  $\lambda_{2,3}$  become dominant, in replace of the pattern  $\lambda_1$ . At the same time, the weights of the patterns  $\lambda_{4,5}$  also increase. The disappearance of the pattern  $\lambda_1$  can be considered as a second-order QPT, which is well-established in literature; (iii) The patterns  $\lambda_{2,3}$ , and additional  $\lambda_{4,5}$  for  $L = 12$  have successively a dominant role in the intermediate regime of the frustration parameter  $\kappa$ , which correspond to two and four domains/kinks, respectively; (iv) the development is ended by the patterns  $\lambda_{4,5}$  for  $L = 8$  or  $\lambda_{6,7}$  for  $L = 12$ , which are identified as the antiphase, namely, the alter-

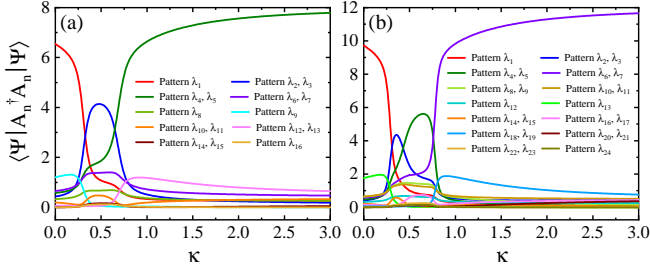


FIG. 4. (a) The patterns' occupancy in the ground state of the system with  $L = 8$  and (b)  $L = 12$  as functions of the frustration parameter  $\kappa$ . The step of  $\kappa$  is 0.003.

native up-up and down-down spins configuration determined by the high frustration parameter  $\kappa$ . The end of such a development is clearly associated with a second-order QPT, which is also well-established in literature; (v) these two second-order QPTs are clearly indicated in the second derivatives of the ground state energies, as shown in the insets of Fig. 3 (b1) and (b2), while those of their pattern components show more dramatically how the QPTs evolve; (vi) in this sense, it is somehow difficult to state that the replacements of the patterns in the intermediate regime of the frustration parameter  $\kappa$  are phase transitions, although there is a small signal when the patterns  $\lambda_{2,3}$  are replaced by the patterns  $\lambda_{4,5}$ . We would like to call them as crossovers, in which two, four, six,  $\dots$ , domains/kinks develop progressively, dependent of the lattice size  $L$ ; (vii) thus in the language of the patterns presented here the phase diagram of the 1D ANNNI model with PBC could be inferred to contain two phases and a crossover regime, where these two phases are the ferromagnetic one and the antiphase and the crossover corresponds to two, four, six,  $\dots$ , domains/kinks, dependent of the lattice size and the frustration parameter  $\kappa$ . Identifications of the paramagnetic phases (I and II in the literature) and the floating phase through the analysis of the correlation function behaviors are insufficient since the nature of this regime is that there are different domains/kinks, which can not be identified as certain phase.

The above analysis can also be confirmed by histograms of the patterns' occupancy calculated by  $\langle \Psi | \hat{A}_n^\dagger \hat{A}_n | \Psi \rangle$  where  $|\Psi\rangle$  is the ground state wavefunction of the system, as shown in Fig. 4. For  $g = J = 1$ , the system is obviously in the ferromagnetic phase, e.g., see Ref. [30], as shown in Fig. 4 (a) and (b) for  $\kappa = 0$ , in which the pattern  $\lambda_1$  dominates over the others. Increasing  $\kappa$ , the pattern  $\lambda_1$  is suppressed gradually, and up to  $\kappa = 0.4$  it already loses its dominant role, which is replaced by the patterns  $\lambda_{2,3}$ . Up to  $\kappa = 0.7$  for  $L = 8$ , the dominant patterns become those of  $\lambda_{4,5}$  as the final stable ground state of the system. Up to  $\kappa = 0.5$  for  $L = 12$ , the dominant patterns become  $\lambda_{4,5}$ , and fur-

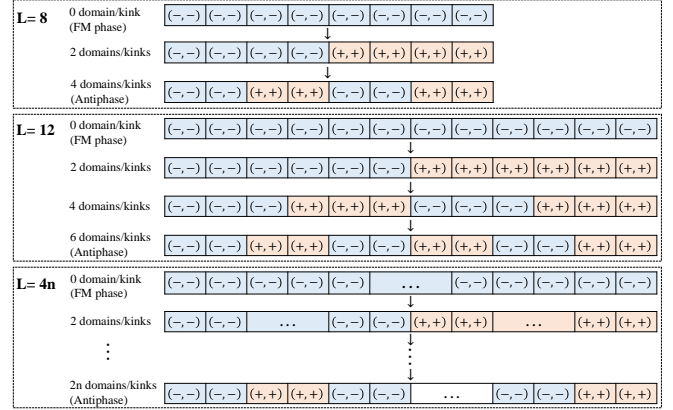


FIG. 5. An inference of the pattern picture to determine the dominant pattern in the ground state of the system with different lattice size  $L = 4n$  ( $n$ : natural number) as increasing the frustration parameter  $\kappa$ . These two patterns  $\lambda_1$  and  $\lambda_{2n}$  have clear definitions of phase: the ferromagnetic (FM) phase and the antiphase with alternative up-up and down-down spins configuration. The intermediate regime contains successively two, four, six,  $\dots$ , domains/kinks, which is a crossover regime, rather than some explicit phases.

thermore, the patterns  $\lambda_{6,7}$  replace those of  $\lambda_{4,5}$  as the final stable ground state of the system. The above observations clearly indicate how the QPTs/crossovers take place, which is in complete agreement with the analysis of the energy components.

*Summary and Discussion.*—We use Fig. 5 to summarize our results. For the lattice size  $L = 8$  and 12, we explicitly analyze what roles the patterns obtained play in the ground state of the 1D ANNNI model under PBC with the frustration parameter  $\kappa$ . The system evolves from the ferromagnetic phase at low frustration to the antiphase at high frustration, in which two second-order QPTs associated with the disappearance of the ferromagnetic phase and the occurrence of the antiphase, respectively, and in the intermediate frustration a crossover rather than some clear phases is addressed. The results are generalized to the system with large lattice size  $L = 4n$  ( $n > 3$ ), which deserves further exploration in order to fix explicitly the phase diagram.

The above results are helpful to clarify the controversial issues reported in the literature. For example, about the number of phases in the 1D ANNNI model [15–18]. Three, four, five, even infinite phases in the thermodynamical limit have been addressed. On the contrary, our suggestion is two phases (the ferromagnetic phase and the antiphase) plus one crossover regime, which contains two, four, six,  $\dots$ , domains/kinks dependent of the frustration parameter  $\kappa$  and lattice size  $L$ . A more detailed study based on some partial information for example the correlation functions is obviously complex, as a consequence, the controversial issues occur naturally. Anyhow, our re-

sults clearly indicate what the intermediate frustration regime looks and different number of domains/kinks dependent of the frustration parameter  $\kappa$  and lattice size  $L$  are involved in such a regime. Our results could be generalized to the frustration physics in high dimensions, which are left for future study.

*Acknowledgments.*—The work is partly supported by the National Key Research and Development Program of China (Grant No. 2022YFA1402704) and the programs for NSFC of China (Grant No. 11834005, Grant No. 12247101).

---

\* luohg@lzu.edu.cn

- [1] A. P. Ramirez, Strongly geometrically frustrated magnets, *Annual Review of Materials Science* **24**, 453 (1994).
- [2] L. Balents, Spin liquids in frustrated magnets, *NATURE* **464**, 199 (2010).
- [3] O. A. Starykh, Unusual ordered phases of highly frustrated magnets: a review, *Reports on Progress in Physics* **78**, 052502 (2015).
- [4] M. Vojta, Frustration and quantum criticality, *Reports on Progress in Physics* **81**, 064501 (2018).
- [5] A. Bar and D. Mukamel, Mixed-order phase transition in a one-dimensional model, *Phys. Rev. Lett.* **112**, 015701 (2014).
- [6] M. Sheinman, A. Sharma, J. Alvarado, G. H. Koenderink, and F. C. MacKintosh, Anomalous discontinuity at the percolation critical point of active gels, *Phys. Rev. Lett.* **114**, 098104 (2015).
- [7] R. Alert, P. Tierno, and J. Casademunt, Mixed-order phase transition in a colloidal crystal, *Proceedings of the National Academy of Sciences* **114**, 12906 (2017).
- [8] P. Scholl, M. Schuler, H. J. Williams, A. A. Eberharter, D. Barredo, K.-N. Schymik, V. Lienhard, L.-P. Henry, T. C. Lang, T. Lahaye, A. M. Laeuchli, and A. Browaeys, Quantum simulation of 2d antiferromagnets with hundreds of rydberg atoms, *NATURE* **595**, 233+ (2021).
- [9] P. Lajkó and F. Iglói, Mixed-order transition in the antiferromagnetic quantum ising chain in a field, *Phys. Rev. B* **103**, 174404 (2021).
- [10] B. Gross, I. Bonamassa, and S. Havlin, Fractal fluctuations at mixed-order transitions in interdependent networks, *Phys. Rev. Lett.* **129**, 268301 (2022).
- [11] R. J. Elliott, Phenomenological discussion of magnetic ordering in the heavy rare-earth metals, *Phys. Rev.* **124**, 346 (1961).
- [12] M. E. Fisher and W. Selke, Infinitely many commensurate phases in a simple ising model, *Phys. Rev. Lett.* **44**, 1502 (1980).
- [13] P. Bak, Commensurate phases, incommensurate phases and the devil’s staircase, *Reports on Progress in Physics* **45**, 587 (1982).
- [14] W. Selke, The annni model — theoretical analysis and experimental application, *Physics Reports* **170**, 213 (1988).
- [15] F. K. Fumani, S. Nemati, and S. Mahdavi, Quantum critical lines in the ground state phase diagram of spin-1/2 frustrated transverse-field ising chains, *Annalen der Physik* **533**, 2000384 (2021).
- [16] S. Nemati, F. Khastehdel Fumani, and S. Mahdavi, far, Comment on “quantum fidelity approach to the ground-state properties of the one-dimensional axial next-nearest-neighbor ising model in a transverse field”, *Phys. Rev. E* **102**, 016101 (2020).
- [17] O. F. d. A. Bonfim, B. Boechat, and J. Florencio, Reply to “comment on ‘quantum fidelity approach to the ground-state properties of the one-dimensional axial next-nearest-neighbor ising model in a transverse field’ ”, *Phys. Rev. E* **102**, 016102 (2020).
- [18] O. F. d. A. Bonfim, B. Boechat, and J. Florencio, Quantum fidelity approach to the ground-state properties of the one-dimensional axial next-nearest-neighbor ising model in a transverse field, *Phys. Rev. E* **96**, 042140 (2017).
- [19] A. Dutta and D. Sen, Gapless line for the anisotropic heisenberg spin  $-\frac{1}{2}$  chain in a magnetic field and the quantum axial next-nearest-neighbor ising chain, *Phys. Rev. B* **67**, 094435 (2003).
- [20] H. Rieger and G. Uimin, The one-dimensional annni model in a transverse field: analytic and numerical study of effective hamiltonians, *Zeitschrift für Physik B Condensed Matter* **101**, 597 (1996).
- [21] A. K. Chandra and S. Dasgupta, Floating phase in the one-dimensional transverse axial next-nearest-neighbor ising model, *Phys. Rev. E* **75**, 021105 (2007).
- [22] A. Nagy, Exploring phase transitions by finite-entanglement scaling of mps in the 1d annni model, *New Journal of Physics* **13**, 023015 (2011).
- [23] C. M. Arizmendi, A. H. Rizzo, L. N. Epele, and C. A. García Canal, Phase diagram of the annni model in the hamiltonian limit, *Zeitschrift für Physik B Condensed Matter* **83**, 273 (1991).
- [24] P. Sen, S. Chakraborty, S. Dasgupta, and B. K. Chakrabarti, Numerical estimate of the phase diagram of finite annni chains in transverse field, *Zeitschrift für Physik B Condensed Matter* **88**, 333 (1992).
- [25] M. Beccaria, M. Campostrini, and A. Feo, Density-matrix renormalization-group study of the disorder line in the quantum axial next-nearest-neighbor ising model, *Phys. Rev. B* **73**, 052402 (2006).
- [26] M. Beccaria, M. Campostrini, and A. Feo, Evidence for a floating phase of the transverse annni model at high frustration, *Phys. Rev. B* **76**, 094410 (2007).
- [27] P. Sen, Application of the interface approach in quantum ising models, *Phys. Rev. B* **55**, 11367 (1997).
- [28] P. R. C. Guimarães, J. a. A. Plascak, F. C. Sá Barreto, and J. a. Florencio, Quantum phase transitions in the one-dimensional transverse ising model with second-neighbor interactions, *Phys. Rev. B* **66**, 064413 (2002).
- [29] J. M. Kosterlitz and D. J. Thouless, Long range order and metastability in two dimensional solids and superfluids. (application of dislocation theory), *Journal of Physics C: Solid State Physics* **5**, L124 (1972).
- [30] Y.-T. Yang and H.-G. Luo, Dissecting Quantum Phase Transition in the Transverse Ising Model, arXiv e-prints , arXiv:2212.12702 (2022).
- [31] Y.-T. Yang and H.-G. Luo, First-Order Excited-State Quantum Phase Transition in the Transverse Ising Model with a Longitudinal Field, arXiv e-prints , arXiv:2301.02066 (2023).
- [32] Y.-T. Yang and H.-G. Luo, Pattern Description of Quantum Phase Transitions in the Transverse Antiferromagnetic Ising Model with a Longitudinal Field, arXiv e-prints , arXiv:2301.05040 (2023).